

# Nonparametric estimation of the preferential attachment function from one network snapshot

Thong Pham  \*<sup>1</sup>, Paul Sheridan  <sup>2</sup>, and Hidetoshi Shimodaira   
1,3

<sup>1</sup>RIKEN Center for AIP

<sup>2</sup>Tupac Bio, Inc.

<sup>3</sup>Kyoto University

June 8, 2024

## Abstract

Measuring preferential attachment in growing networks has received considerable attention, not only for understanding how heavy-tail degree distributions emerge in real-world networks, but also for gaining insight into various rich-get-richer effects that arise in diverse fields. Conventional estimation methods require that a network be observed across at least two snapshots in time. Numerous real-world datasets are, however, available only as single snapshots, rendering most conventional methods inapplicable of estimating a general preferential attachment function. We propose a nonparametric method, called PAFit-oneshot, for estimating preferential attachment in a growing network from one snapshot. PAFit-oneshot corrects for a previously unnoticed bias that arises when estimating preferential attachment values only for degrees observed in the snapshot. Our work provides scientists with a means of measuring preferential attachment in a large number of publicly available one-snapshot networks. As a demonstration, we estimated preferential attachment in three such networks, and found sublinear preferential attachment in all cases.

*Keywords:* preferential attachment, growing networks, nonparametric estimation

## 1 Introduction

One of the biggest discoveries in network science is surprising universality of heavy-tail degree distributions in real-world networks. They show up in both human-made

---

\*Corresponding author. Email: thong.pham@riken.jp

and natural networks in the domains of technology, biology, society, and even linguistics [42, 27, 37]. Historically, the discussion about heavy-tail degree distributions in the literature had centered around power-laws [2], until it was pointed out in more recent times that heavy-tails can take on a rich variety of forms [8, 20]. The stretched-exponential, log-normal, power-law with cut-off, stretched exponential with cut-off, and are all examples of heavy-tailed distributions that have been observed in real-world networks. Estimating the correct functional form of a heavy-tail degree distribution is an active area of research in network science [42, 45, 44, 37], and new computational tools are being introduced [12].

To explain the widespread presence of heavy-tail degree distributions, network scientists employ the concept of preferential attachment (PA). According to this mechanism, the probability a node with degree  $k$  acquires a new edge is proportional to  $A_k$ , the “attachment” value degree  $k$  nodes.

In using PA, it turns out that network scientists are standing on the shoulders of giants; namely, PA is closely related to various self-reinforcing mechanisms that have been found to be important in a wide range of fields. The first instance of such mechanisms arose in biology when the Yule process was proposed to describe the evolution of biological species [46]. Simon employed the same concept to explain various phenomena, not only in biology, but also in sociology and economics [39]. Merton coined the now-famous term “Matthew effect” when he used the PA concept to explain the discrepancies in recognition between famous scientists and less-known ones [23]. In scientometrics, Price used the phrase “cumulative advantage” when referring to the PA mechanism that he employed in a series of papers [31, 32] to explain not only the tendency in which currently heavily cited papers tend to be cited more frequently, but also Lotka’s law in scientific productivity [21] and Bradford’s law in journal use [6]. PA was also recently used in describing the herding effect in financial markets [35].

The function  $A_k$  is often called *attachment kernel* or *attachment function*. When  $A_k$  is equal to  $k + c$ , we have the celebrated linear preferential attachment function, the first PA function investigated by the complex network community [2]. The PA phenomenon in real-world networks can, however, come in a great variety of forms. Estimating the PA function from a given real-world network is important not only for verifying various assumptions about how heavy-tail degree distributions arise, but also for providing new insights on the aforementioned related phenomena in various fields.

The problem of estimating  $A_k$  has traditionally been considered in the setting when the growth process of a network is observed [24]. Consider a network that grows from time  $t = 1$  to  $T$ . Denote its snapshot at time  $t$  by  $G_t$ . A number of methods for estimating the  $A_k$  function of a growing network when at least some of its snapshots are observed have been proposed [15, 24, 28].

However, what if we cannot observe anything about the growth process and have to contend ourselves with only the final snapshot  $G_T$ ? Is it possible to recover  $A_k$ , a function that governs the growth process, without observing the growth process itself? When it comes to estimating PA without any time-resolved data, no satisfactory methods exist. All existing methods assume either unrealistic network types or unnecessarily restrictive functional forms for  $A_k$  [4, 38, 13, 43, 11, 7].

Solving this problem potentially has enormous impact on account of the vast number of one-snapshot, real-world complex network datasets that exist in online databases. Such a method would allow researchers to uncover new insights on PA and various related phenomena that are currently buried in those one-snapshot networks.

Our contributions are two-fold. In our main contribution, we propose a method called PAFit-oneshot to nonparametrically estimate the PA function of a growing network from its final snapshot,  $G_T$ , alone. Our method does not assume any functional form for the PA function, and can be applied to any real-world network snapshot.

At the heart of our solution is a correction for a bias that occurs when the PA function is nonparametrically estimated from one snapshot. Since one always estimates the PA values of the degrees  $k$  that exist in the snapshot, the numbers of nodes with those degrees are always positive *a priori*. Failing to account for this bias leads to what may be called a waterfall artefact; that is, a severe underestimation of  $A_k$  in the region of large  $k$ , as we illustrate in Fig. 1. Surprisingly, the presence of this bias, let alone its correction, has to our knowledge never been discussed in the literature.

To remove this bias, we show that, for each degree  $k$  that exists in a network snapshot, we need to estimate the probability of its existence in the snapshot, i.e., the probability that we observe  $k$  in  $G_T$ . This resembles the problem of post-selection inference, which is also known as selective inference [40, 41]. Post-selection inference typically considers model selection in a regression setting and adjusts the bias of regression coefficients for the selected predictors; one must correct for the effect of choosing the predictor. In our problem, model selection is equivalent to choosing over which range of  $k$  to estimate  $A_k$ , which is where  $k$  exists in  $G_T$ .

Since the probability that  $k$  exists in  $G_T$  is not readily available from the observed snapshot, we use a two-step procedure to estimate it. First, we calculate a rough estimation of  $A_k$ . While this estimate is plagued by the bias in the region of large  $k$ , its values in the region of small  $k$  are reasonably accurate. Then we use this roughly estimated  $A_k$  to simulate multiple networks and estimate the needed quantities by their averages in these simulated networks. Intuitively speaking, we leverage the good quality of the small degree part to improve the large degree part, using the dynamics of the growth model as a lever. The proposed method is implemented in the R package PAFit [30].

In our second contribution, in Section 5, we applied the proposed method to three real-world networks without growth information, and obtained sublinear PA functions in all three cases. Since these networks do not contain time-resolved data, it had been impossible to estimate PA functions of these networks until now. The sublinear functions are considerably weaker than the conventional linear PA form  $A_k = k + c$  which is often employed in modelling one-snapshot networks [4, 43] or as similarity index in link predictions [22]. This emphasizes the need to look beyond the conventional linear PA in one-snapshot networks.

## 2 Model and Proposed Method

After introducing the network model in Section 2.1, we provide the theoretical foundation in Section 2.2. We then introduce a baseline method in Section 2.3 and present our proposed method in Section 2.4. Finally, we demonstrate our method through an example in Section 2.5.

### 2.1 The Simple Growth model

The method assume the Simple Growth (SG) network model, which is flexible enough for modelling various real-world networks. The model is directed and starts at time  $t = 1$  with two isolated nodes. At each time-step  $t$ , to form  $G_{t+1}$ , we add to  $G_t$  either a new isolated node with probability  $p(t)$  or a new edge between existing nodes with probability  $1 - p(t)$ . In the latter case, the destination node is chosen based on the PA rule: a node with in-degree  $k$  is chosen with probability proportional to  $A_k$ . The quantity  $p(t)$  is a deterministic number in  $(0, 1)$ . It is sometimes called an edge-step function [3].

Unlike tree models, the SG model can model realistic real-world networks. A network generated by the SG model is typically not a tree, since there can be a new edge between existing nodes at each time-step, which can create cycles. The expected proportion of the numbers of nodes and edges  $h(t) = \mathbb{E}[N(t)/E(t)]$  in our model is approximately  $\sum_{i=1}^{t-1} p(i)/(t - 1 - \sum_{i=1}^{t-1} p(i))$ , which can be tuned to be any positive value.

In this paper we are only interested in the PA phenomenon related to the in-degree distribution of a network. Therefore, we do not explicitly model how source nodes are selected and assume only that, conditional on  $G_t$ , source node selection is independent of how the destination node is chosen. Furthermore, unless stated otherwise, all degree-related quantities should be understood to refer to in-degree.

### 2.2 A formula for estimating $A_k$ from one snapshot

Let  $n_k(t)$  be the number of nodes with degree  $k$  at time-step  $t$ . We have the following theorem which is key to the derivation of the PAFit-oneshot method. A proof can be found in Appendix A. Gao et al. [11] provided a similar formula for PA trees.

#### Theorem 1

Assume that  $p(t) = p + O(t^{-1/2} \log t)$  with  $0 < p < 1$ . If  $A_k$  satisfies the conditions stipulated below, then for a fixed  $k$  we have

$$A_k = \lambda \frac{\mathbb{E} \sum_{j>k} n_j(t)}{\mathbb{E} n_k(t)} + o(1), \quad (1)$$

as  $t$  tends to infinity, where  $\lambda$  is some constant that is independent of  $t$  and  $k$ .

For Theorem 1, we assume that

- (a)  $A_k \leq A_{k+1}$  for all  $k$  and,

- (b) There exists a constant  $\eta > 0$  such that  $\mathbb{P}(|H(t)/t - \eta| \geq t^{-1/2} \log t) \leq O(t^{-1/2} \log t)$ , with  $H(t) = \sum_k A_k n_k(t)$ .

The first assumption means that  $A_k$  is a non-decreasing function, which is true for the power-law form  $A_k = k^\alpha$  with  $\alpha \geq 0$  or the linear form  $A_k = k + c$  with  $c > 0$ . This assumption has also been used in previous PA network models [14, 10]. While we need this assumption for our convergence proof, PAFit-oneshot does not actually employ this assumption in its procedure and, based on our experience, works even when the true PA function is not monotone.

The second assumption implies that  $H(t)/t$  converges to some constant  $\eta$ . We note that the actual value of  $\eta$  is not needed for estimating  $A_k$ . This assumption is needed in order to handle the normalizing factor  $H(t)$ . A similar version of this assumption has been used previously [17]. The assumption is satisfied, for example, by  $A_k = k + c$  with  $\eta = 1 + (c - 1)p$  or  $A_k = 1$  with  $\eta = 1 - p$ . Note that in these two cases,  $\mathbb{P}(|H(t)/t - \eta| \geq t^{-1/2} \log t) \leq O(t^{-b})$  for any positive constant  $b$ , which is a much stronger rate than what is assumed in the second assumption.

### 2.3 A baseline method

We can derive an estimation method for  $A_k$  from Eq. (1). Assuming that  $T$  is large enough, we obtain:

$$A_k \approx \lambda \frac{\mathbb{E} \sum_{j>k} n_j(T)}{\mathbb{E} n_k(T)}, \quad (2)$$

with  $\lambda$  being a constant that is independent of  $k$  and hence can be ignored. One then estimates  $\mathbb{E} \sum_{j>k} n_j(T)$  and  $\mathbb{E} n_k(T)$  by  $\sum_{j>k} n_j(T)$  and  $n_k(T)$ , respectively. This yields the baseline method:

$$\hat{A}_k^{\text{baseline}} = \frac{\sum_{j>k} n_j(T)}{n_k(T)}. \quad (3)$$

While this estimator works very well for small  $k$ , for large  $k$  it suffers from the waterfall artefact: the estimated values of  $A_k$  fall off rapidly (cf. Fig. 1). To our knowledge, while this estimator has been proposed for PA trees by Gao et al. [11], it has never been applied to any real-world networks, and the waterfall artefact, let alone its cause, has never been discussed in the literature.

### 2.4 New method for estimating $A_k$ from one snapshot: PAFit-oneshot

We present our main contribution: the novel method PAFit-oneshot for estimating  $A_k$  when only  $G_T$ , the snapshot at time-step  $T$ , is observed. At the heart of our method is a correction to the waterfall artefact inherent to Eq. (3).

The root of the waterfall artefact is that  $n_k(T)$  is not a good estimator of  $\mathbb{E} n_k(T)$  when  $k$  is large. Given  $G_T$ , we only estimate the  $A_k$  values for the degrees  $k$  observed in  $G_T$ , which means  $n_k(T)$  is positive *a priori*. Therefore,  $n_k(T)$  is actually an estimator for the conditional expectation  $\mathbb{E}[n_k(T) | n_k(T) > 0]$ , which

is equal to  $\mathbb{E}n_k(T)/\mathbb{P}(n_k(T) > 0)$ . Correcting for  $p_k := \mathbb{P}(n_k(T) > 0)$  leads us to the following equation:

$$A_k \approx \frac{\sum_{j>k} n_j(T)}{n_k(T)p_k}. \quad (4)$$

Since  $A_k$  is only identifiable up to a multiplicative constant, were the  $p_k$  values the same for all  $k$ , Eq. (4) would be equivalent to Eq. (2). However, since  $p_k$  tends to decrease rapidly when  $k$  is large (cf. Fig. 1b), the correction in Eq. (4) is necessary.

Correcting for the probability of observing  $k$  resembles the problem of post-selection inference [40, 41]. Post-selection inference adjusts for bias that crops up from the act of parameter selection. One often achieves the bias-correction by changing all probabilities in the subsequent data analysis to conditional probabilities that are conditioned on the selection event. In our problem for estimating  $A_k$ , we consider the conditional probabilities given that the degree  $k$  is observed in  $G_T$ , i.e.,  $n_k(T) > 0$ .

We estimate  $p_k$  via  $S$  ( $S \geq 1$ ) rounds of simulations for sequentially updating  $\hat{A}_k^{(s)}$  and  $\hat{p}_k^{(s)}$ ,  $s = 1, \dots, S$ . We start with the same baseline estimator in Eq. (3), which is equivalent to initially estimating  $p_k \propto 1$  in Eq. (4). In particular, we define  $\hat{A}_k^{(0)}$ , the initial estimate of our iterative procedure, to be equal to  $\hat{A}_k^{\text{baseline}}$ . At each round  $s = 1, \dots, S$ , we use  $\hat{A}_k^{(s-1)}$  as the true PA function and simulate  $M$  networks. We see whether the degree  $k$  exists at time-step  $T$  in the  $i$ -th simulated network:

$$p_k^{(s,i)} := \mathbf{1}_{n_k(T)^{(s,i)} > 0}, \quad (5)$$

and estimate  $\hat{p}_k^{(s)}$  by the average of the  $p_k^{(s,i)}$ 's:

$$\hat{p}_k^{(s)} := \frac{1}{M} \sum_{i=1}^M p_k^{(s,i)}. \quad (6)$$

When simulating SG model networks, we assume that  $p(t) = \hat{p}$  with  $\hat{p} = (N - 2)/(E + N - 2)$ , where  $N$  and  $E$  are the numbers of nodes and edges in the observed network  $G_T$ , respectively. At the end of round  $s$ , we update  $\hat{A}_k^{(s)}$  using Eq. (4) with the current value of  $\hat{p}_k^{(s)}$ :

$$\hat{A}_k^{(s)} = \frac{\sum_{j>k} n_k(T)}{n_k(T)\hat{p}_k^{(s)}}. \quad (7)$$

After  $S$  rounds, the estimate for  $p_k$  is the average of the  $\hat{p}_k^{(s)}$ 's:

$$\hat{p}_k := \frac{1}{S} \sum_{s=1}^S \hat{p}_k^{(s)}. \quad (8)$$

For additional stability, we repeat the whole process five times to obtain five values of  $\hat{p}_k$  and use their average, denoted as  $\hat{p}_k^{\text{final}}$ , as the final estimate of  $p_k$ . The final estimate of  $A_k$  is:

$$\hat{A}_k = \frac{\sum_{j>k} n_k(T)}{n_k(T)\hat{p}_k^{\text{final}}}. \quad (9)$$

The number of simulated networks,  $M$ , in each round and the number of simulation rounds,  $S$ , are parameters in PAFit-oneshot. In our experience, while an  $M$  of around 100 is enough, a small value of  $S$ , for example,  $S = 5$ , is stable.

A schematic presentation of PAFit-oneshot is given in Fig. 6. In order to avoid clutter, we leave the binning version of the method to Appendix B.

## 2.5 An illustrative example

Figure 1 showcases our method through a simple simulated example that uses the linear PA function  $A_k = \max(k, 1)$  as the true PA function. The underlying network was generated by the SG model with  $p(t) = 0.5$  and  $T = 50000$ . We applied PAFit-oneshot with  $M = 200$  and  $S = 5$ .

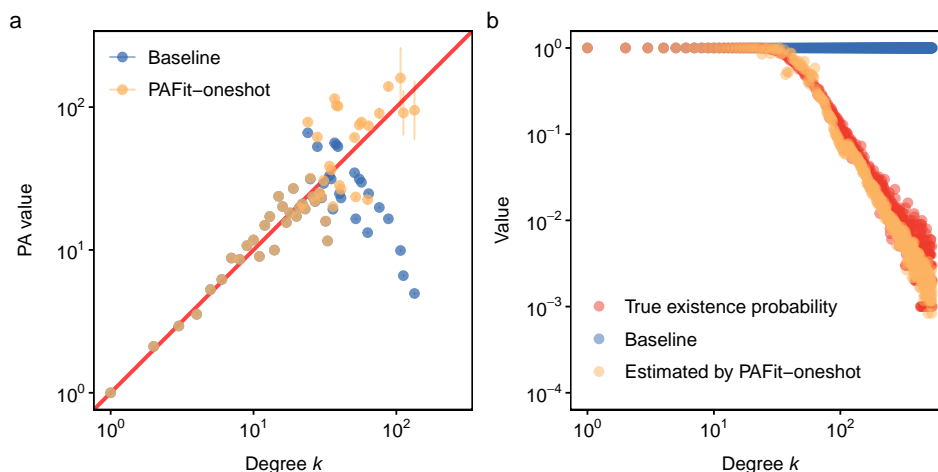


Figure 1: Estimating  $A_k$  from one network snapshot of an SG model generated network with true PA function is  $A_k = \max(k, 1)^\alpha$  with  $\alpha = 1$ . **Panel a:** The proposed method (yellow dots) corrects the waterfall artefact in the baseline method estimate (blue dots). The bar at each yellow dot depicts the plus/minus two-sigma confidence interval estimated by the proposed method. The true PA function is shown as a red line for reference. We obtained  $\hat{\alpha}_{\text{baseline}} = 0.52 (\pm 0.19)$  and  $\hat{\alpha}_{\text{PAFit-oneshot}} = 0.93 (\pm 0.08)$ ; the confidence interval for  $\hat{\alpha}$  is plus/minus two-sigma. **Panel b:** PAFit-oneshot improves upon the baseline in estimating  $p_k = \mathbb{P}(n_k(T) > 0)$ . The true  $p_k$  is calculated from 1000 simulated SG model networks. For ease of visualization, all the series are scaled so that the value of each series at  $k = 1$  is 1.

Figure 1a shows that PAFit-oneshot accurately recovers the true PA function. By contrast, the baseline estimate given by Eq. (3) performs well when  $k$  is small, but is plagued by the waterfall artefact when  $k$  is large. To our knowledge, no principled way to automatically determine where the waterfall artefact starts to kick in has yet been devised. Due to this artefact, estimating  $\alpha$  using the least

square method from the entire range of the estimation result  $\hat{A}_k$  leads to a severely underestimated value:  $\hat{\alpha}_{\text{baseline}} = 0.52 (\pm 0.19)$ .

This artefact occurs since the baseline method does not take into account the *a priori* existence of the degree  $k$  nodes in the snapshot. The cause of the waterfall artefact is that the baseline method over-estimates  $p_k$  for large  $k$ . Using a simulation step to estimate  $p_k$  leads to better estimation of  $p_k$ , as can be seen in Fig. 1b. Using a weighted least square method, we obtain  $\hat{\alpha}_{\text{PAFit-oneshot}} = 0.93 (\pm 0.08)$ .

### 3 Simulation Study

We investigate the performance of PAFit-oneshot in two types of simulations: in Section 3.0.1,  $p(t)$  is held fixed, while in Section 3.0.2  $p(t)$  varies based on real-world data.

To generate networks, we use the power-law yielding form  $A_k = \max(k, 1)^\alpha$ , which has been used frequently in previous works. We investigate five values of  $\alpha$ : 0, 0.25, 0.5, 0.75, and 1. From the estimation value  $\hat{A}_k$  of each method, we estimate  $\alpha$  and use the quality of the result as a proxy to judge how well each method estimates  $A_k$ . To estimate  $\alpha$  from  $\hat{A}_k$ , we employ least squares for the baseline method, and a weighted least squares method for PAFit-oneshot, since this method provides standard deviations for the individual  $\hat{A}_k$  values.

An advantage of our nonparametric approach is that we do not need to pre-specify a functional form for  $A_k$ ; one can simply fit a specific form to the estimated value  $\hat{A}_k$ . Beside the power-law form, in Appendix D we use another functional form as the true PA function.

#### 3.0.1 Constant $p(t)$

In this section, we assume  $p(t) = p$  and test three values of  $p$ :  $p = 0.05$ ,  $p = 0.1$ , and  $p = 0.5$ . These values are similar to the average values of  $p(t)$  observed in real-world networks (see Tables 2 and 3). A total of 50 networks were simulated for each value of  $p$ . The total number of time-steps in each network is  $T = 5 \times 10^5$ . The estimation result for each  $\alpha$  is shown in Fig. 2.

The proposed method outperforms the baseline method in all settings, since the baseline method severely underestimate  $\alpha$  due to the waterfall artefact. PAFit-oneshot underestimates  $\alpha$  when  $\alpha$  is near 1 and  $p = 0.05$ . When  $p$  is small, there will be more new edges and less new nodes added to the network. This will often increase the maximum degree in the network when  $\alpha$  is near 1, which makes the estimation harder since there are more  $A_k$  values to be estimated. Interestingly, the same phenomenon has been observed in estimating the PA function with full time information [28, 29, 30]. Taking also the results in Fig. 7 into consideration, one can then conclude that the proposed method works well and outperforms the baseline when  $p(t)$  is constant.

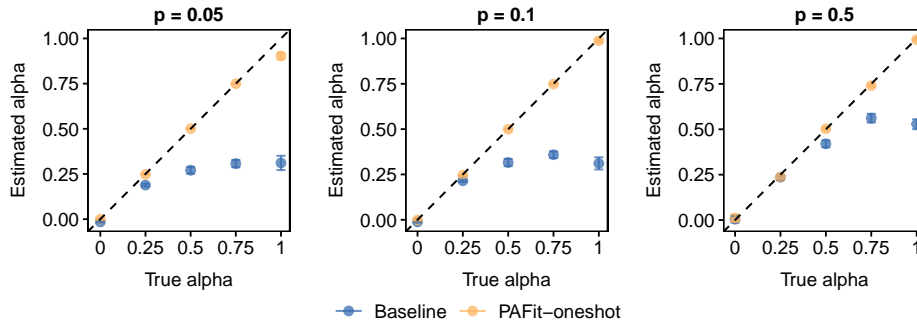


Figure 2: Estimated  $\alpha$  from  $\hat{A}_k$ . For each case,  $p(t) = p$ , i.e., a constant. The network has  $T = 5 \times 10^5$  and  $A_k = \max(k, 1)^\alpha$  as the true PA function. In each combination of the parameters  $p$  and  $\alpha$ , for each method we plot the mean of the estimated  $\alpha$  and its plus/minus two-sigma confidence interval obtained from 50 simulated networks.

### 3.0.2 Varying $p(t)$

Here we check by simulations the robustness of the proposed method, which assumes  $p(t) = p$  for the simulation step, in real-world situations when  $p(t)$  varies over time. In this simulation, at each time-step, we added a new node or a new edge according to a node-edge sequence taken from a real-world network, and only sampled where the new edge connects based on the PA rule  $A_k = \max(k, 1)^\alpha$ . We used three networks: the Enron email network [16], the Escort rating network [34], and the UC Irvine forum message network [26]. Some of their statistics can be found in Table 2.

In all three networks, the estimated  $p(t)$  function varies greatly, as can be seen from Fig. 10. While the  $p(t)$  series in the Escort network and the UC Irvine network start high then rapidly decrease to some stable value around 0.1, the series of Enron networks, while decreasing from a high starting value, show great fluctuations even toward the end of the growth process.

The results of the simulation are shown in Fig. 3. The proposed method again outperforms the baseline. Although there are some performance degradation as expected, PAFit-oneshot performs reasonably well in the region of moderate to large PA effect ( $0.75 \leq \alpha \leq 1$ ) in all three networks. Figures 9a and b show two runs which are typical for the situations when  $\alpha$  is small and when  $\alpha$  is large, respectively, in the Enron network. When  $\alpha$  is small, PAFit-oneshot fails to remove the waterfall artefact and behaves similarly to the baseline method. When  $\alpha$  is large, the proposed method successfully removes the waterfall artefact and estimate the PA function comparatively well. Taking also the results in Fig. 8 into account, we conclude that when  $p(t)$  is varying, the proposed method outperformed the baseline method in all settings and is reasonably good in the region of moderate to large PA effect.

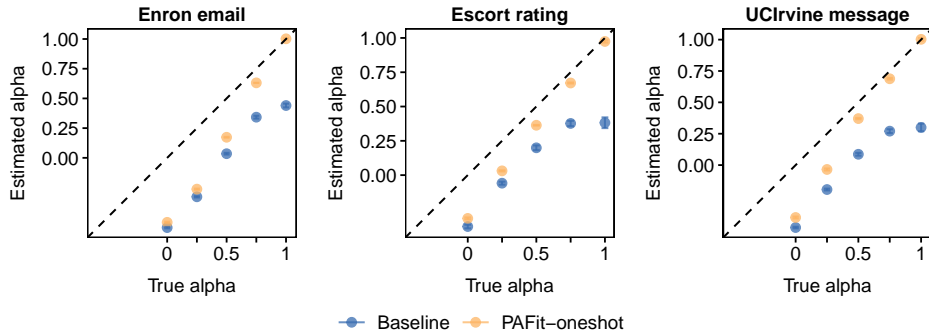


Figure 3: Estimated  $\alpha$  from  $\hat{A}_k$ . We used node-edge sequences obtained from real-world networks and  $A_k = \max(k, 1)^\alpha$ . In each setting, for each method we plot the mean of the estimated  $\alpha$  and its plus/minus two-sigma confidence interval obtained from 50 simulated networks.

#### 4 The method recovers the true PA functions in time-resolved real-world networks

We compare the proposed method with the Maximum Likelihood Estimation (MLE), explained in Appendix C. The MLE can be viewed as the gold standard approach when fully time-resolved data is available. We used the three real-world networks we introduced in Section 3.0.2: the Enron email, the Escort rating, and the UC Irvine forum message networks. For each network, we apply PAFit-oneshot with  $M = 50$  and  $S = 5$ . The results are shown in Figure 4.

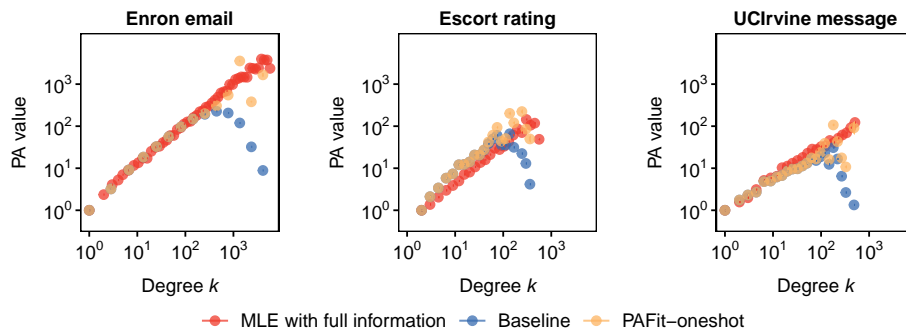


Figure 4: Estimation results in real-world networks when the time-step information is available.

Compared to the MLE with full information, PAFit-oneshot and the baseline estimated  $A_k$  reasonably well when  $k$  is small. When  $k$  is large, the baseline, however, severely underestimated  $A_k$  as expected. The proposed method did not suffer from the bias and estimated  $A_k$  reasonably well even when  $k$  is large.

Since all the estimated PA functions in three networks appear to be power-law, we fitted the functional form  $A_k = \max(k, 1)^\alpha$  to the estimated  $A_k$  and estimated the attachment exponent  $\alpha$  (Table 1) by weighted least squares. Overall, the proposed method agrees reasonably well with the MLE with full time information on the estimated value of  $\alpha$ .

Table 1: Estimated  $\alpha$  in real-world networks with time-resolved data. Each confidence interval of the estimated  $\alpha$  is plus/minus two-sigma. The functional form  $A_k = \max(k, 1)^\alpha$  is fit to  $\hat{A}_k$  by weighted least squares.

Estimation Method	Enron email	Escort rating	UCIrvine message
MLE with full time information	$0.93 \pm 0.02$	$0.92 \pm 0.03$	$0.74 \pm 0.03$
PAFit-oneshot	$1.01 \pm 0.05$	$1.07 \pm 0.09$	$0.67 \pm 0.04$
Baseline	$0.42 \pm 0.3$	$0.57 \pm 0.3$	$0.28 \pm 0.2$

## 5 The method predicts sublinear PA functions in real-world networks with unknown timelines

We apply PAFit-oneshot to three networks for which no time-resolved data is presently available: a portion of the Google+ user-user network [19], a network of airports in the US [25], and a followship network between political blogs in the 2004 US Election [1]. For more information on these networks, see Appendix F. Since these networks are single-snapshots without time-resolved data, nonparametrically estimating the PA function from them has been impossible up to now. In each network, we apply PAFit-oneshot with  $M = 50$  and  $S = 5$ . The results are shown in Fig. 5.

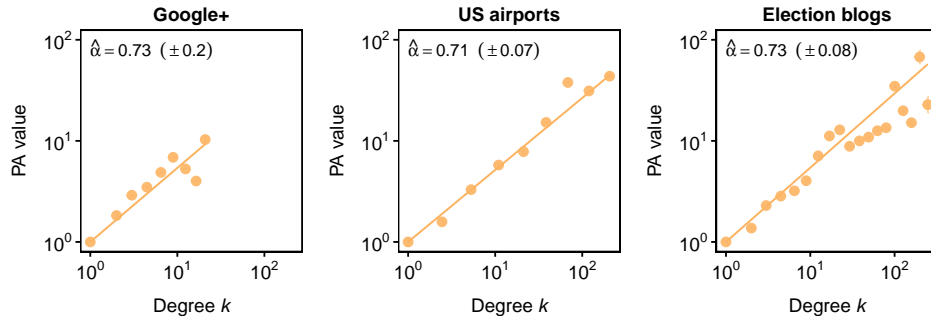


Figure 5: Estimation results in real-world networks with no time-resolved data. The functional form  $A_k = \max(k, 1)^\alpha$  is fit to  $\hat{A}_k$  by weighted least squares. The confidence interval for each estimated  $\alpha$  is plus/minus two-sigma.

The PA phenomenon is present in all networks. Furthermore, since each estimated  $A_k$  is roughly linear on a log-log scale, we fit the functional form  $A_k =$

$\max(k, 1)^\alpha$  and estimate  $\alpha$ . Since all estimated  $\alpha$  is smaller than 1, the PA phenomenon in all three networks is sublinear. The estimated PA functions are significant weaker than the conventional linear form  $A_k = k + c$  which is often employed in modelling one-snapshot networks [4, 43] or as similarity index in link predictions in one-snapshot networks [22]. This emphasizes the need to look beyond linear PA in one-snapshot networks.

## 6 Conclusion

We proposed a novel method, called PAFit-oneshot, for estimating the PA function nonparametrically from a single network snapshot. The key to our method is a correction of a previously unnoticed bias that has a connection with post-selection inference. We demonstrated that PAFit-oneshot recovers the PA function reasonably well under realistic settings. By applying PAFit-oneshot to three real-world networks without time-resolved data, we found the first evidence for the presence of sublinear PA in real-world, non-time-resolved network data.

On the theoretical front, there are various directions for future research. One important direction is to rigorously quantify the effect of the simulation step, which is needed in our method for correcting the selective bias. Another interesting direction is to try to bypass this step entirely. This would require an explicit formula that is not only calculable from one snapshot, but is also unaffected by the bias. A starting point may be to study the non-asymptotic properties of the  $p_k$  function. Yet another promising direction is to investigate the presence of selective biases in estimating other network growth mechanisms.

On the application front, our work opens up a path to estimate the PA function in previously out-of-reach one-snapshot networks. It is our hope that the incoming new evidence provides new insights into the connection between the processes underlying complex network evolution and their large-scale topological features.

## Funding

This work was supported by the Japan Society for the Promotion of Science KAKENHI [JP19K20231 to T.P., JP20H04148 to H.S.].

## A Proof of Theorem 1

### A.1 Proof sketch

Theorem 1 is a simple consequence of the following proposition:

#### Proposition 1

*We assume the same assumptions as in Theorem 1. For  $k \geq 0$ , let  $\mu_k$ 's be the constants that satisfy*

$$\mu_k = \lambda^{-1}(A_{k-1}\mu_{k-1} - A_k\mu_k) + \mathbf{1}_{k=0}, \quad (10)$$

with  $\lambda = \eta(1-p)^{-1}$  and with the convention that  $A_{-1} = \mu_{-1} = 0$ . For a fixed  $k$ , there exist constants  $M$  and  $T$  such that for all  $j \leq k$ ,  $|\mathbb{E}n_j(t)/(pt) - \mu_j| \leq Mt^{-1/2} \log t$  for all  $t \geq T$ .

Equation (10) is similar to the equation in the case of PA trees [18, 36, 5]. In such trees,  $\eta$  is sometimes called the Malthusian rate of growth and plays an crucial role in the theoretical analysis [5]. Equation (10) can be used to check that  $\sum_k \mu_k = 1$ , i.e., the  $\mu_k$ 's form a probability distribution. The following key equation can be deduced from Eq. (10):

$$\sum_{j>k} \mu_j = \lambda^{-1} A_k \mu_k, \quad (11)$$

for  $k \geq 0$ .

Assuming Proposition 1, one can show Theorem 1 as follows. We have:

$$\begin{aligned} \mathbb{E} \sum_{j>k+1} n_j(t) &= \mathbb{E} \left[ N(t) - \sum_{j=0}^k n_j(t) \right] = \sum_{i=1}^{t-1} p(i) + 2 - \sum_{j=0}^k \mathbb{E}n_j(t) \\ &= (t-1)p + 2 - tp \sum_{j=0}^k \mu_k + O(t^{1/2} \log t) \quad (\text{using Proposition 1}) \\ &= tp \sum_{j>k} \mu_j + O(t^{1/2} \log t) \quad (\text{using } \sum_j \mu_j = 1) \\ &= tp \frac{A_k \mu_k}{\lambda} + O(t^{1/2} \log t) \quad (\text{using Eq. (11)}) \\ &= \frac{A_k \mathbb{E}n_k(t)}{\lambda} + O(t^{1/2} \log t) \quad (\text{using Proposition 1}). \end{aligned}$$

Noting that, from Proposition 1,  $\mathbb{E}n_k(t)$  is positive for sufficiently large  $t$ , we have:

$$\frac{\mathbb{E} \sum_{j>k} n_j(t)}{\mathbb{E}n_k(t)} = \frac{A_k}{\lambda} + \frac{O(t^{1/2} \log t)}{\mathbb{E}n_k(t)} = \frac{A_k}{\lambda} + \frac{O(t^{1/2} \log t)}{tp\mu_k + O(t^{-1/2} \log t)} = \frac{A_k}{\lambda} + O(t^{-1/2} \log t). \quad (12)$$

This concludes the proof of Theorem 1.

Next, we present a sketch of the proof of Proposition 1. Recall that  $H(t) = \sum_k n_k(t) A_k$  is the normalizing factor at time-step  $t$ . We have:

$$\mathbb{E}[n_k(t+1)|G_t] = n_k(t) + (1-p(t))A_{k-1}n_{k-1}(t)/H(t) - (1-p(t))A_k n_k(t)/H(t) + p(t)\mathbf{1}_{k=0}. \quad (13)$$

The quantity  $A_k n_k(t)/H(t)$  is  $O(1)$  for all  $k \geq 0$  and  $t \geq 1$ . The error of approximating  $A_k n_k(t)/H(t)$  by  $A_k n_k(t)/(\eta t)$  is  $\Delta_k = (\eta t - H(t))A_k n_k(t)/H(t)/(\eta t)$ , which is always  $O(1)$ . Due to assumption (b),  $\mathbb{E}\Delta_k = O(t^{-1/2} \log t)$ . The same holds for  $\mathbb{E}\Delta_{k-1}$ .

Taking expectations of both sides of Eq. (13), we then have:

$$\begin{aligned} \mathbb{E}n_k(t+1) &= \mathbb{E}n_k(t) + (1-p(t))A_{k-1}\mathbb{E}n_{k-1}(t)/(\eta t) - (1-p(t))A_k\mathbb{E}n_k(t)/(\eta t) + p(t)\mathbf{1}_{k=0} \\ &\quad + O(t^{-1/2} \log t). \end{aligned} \quad (14)$$

Substituting  $p(t) = p + O(t^{-1/2} \log t)$  into the preceding equation yields:

$$\mathbb{E}n_k(t+1) = \mathbb{E}n_k(t) + \frac{A_{k-1}}{\lambda t} \mathbb{E}n_{k-1}(t) - \frac{A_k}{\lambda t} \mathbb{E}n_k(t) + p\mathbf{1}_{k=0} + O(t^{-1/2} \log t), \quad (15)$$

for all  $k \geq 0$ .

One can show heuristically that Eq. (15) implies Eq. (10) by dividing both sides of Eq. (15) by  $p$  and re-arranging the terms:

$$(t+1) \frac{\mathbb{E}n_k(t+1)}{p(t+1)} - t \frac{\mathbb{E}n_k(t)}{pt} = \lambda^{-1} \left( A_{k-1} \frac{\mathbb{E}n_{k-1}(t)}{pt} - A_k \frac{\mathbb{E}n_k(t)}{pt} \right) + \mathbf{1}_{k=0} + O(t^{-1/2} \log t). \quad (16)$$

If one assumes that  $\lim_{t \rightarrow \infty} \mathbb{E}n_k(t)/(pt)$  exists and is equal to  $\mu_k$ , sending  $t$  to infinity in Eq. (16) yields Eq. (10). While the rigorous argument is more involved, it is standard. For completeness, we include it in the next section.

## A.2 Details

Let  $\epsilon_k(t) = \mathbb{E}n_k(t) - pt\mu_k$ . From Eq. (10):

$$(t+1)p\mu_k = tp\mu_k + p\mu_k = tp\mu_k + p\lambda^{-1}A_{k-1}\mu_{k-1} - p\lambda^{-1}A_k\mu_k + p\mathbf{1}_{k=0} = tp\mu_k + \frac{A_{k-1}}{\lambda t}pt\mu_{k-1} - \frac{A_k}{\lambda t}pt\mu_k + p\mathbf{1}_{k=0}.$$

Subtracting this from Eq. (15) gives us:

$$\epsilon_k(t+1) = \epsilon_k(t) + \frac{A_{k-1}}{\lambda t} \epsilon_{k-1}(t) - \frac{A_k}{\lambda t} \epsilon_k(t) + O(t^{-1/2} \log t), \quad (17)$$

for all  $k \geq 0$ . This means that there exist some constants  $L \geq 0$  and  $t_0 \geq 1$  such that:

$$\left| \epsilon_k(t+1) - \left( 1 - \frac{A_k}{\lambda t} \right) \epsilon_k(t) - \frac{A_{k-1}}{\lambda t} \epsilon_{k-1}(t) \right| \leq Lt^{-1/2} \log t, \quad (18)$$

for all  $t \geq t_0$  and all  $k \geq 0$ .

For a fixed  $k$ , we will prove that there exist constants  $M$  and  $T$ , to be specified later, such that

$$|\epsilon_j(t)| \leq Mt^{1/2} \log t, \quad (19)$$

for  $t \geq T$  and  $0 \leq j \leq k$  by induction on  $t$ . This will prove the assertion.

When  $t = T$ , for all  $j$ , we have  $\epsilon_j(T) \leq \mathbb{E}n_j(T) + pT\mu_j \leq T+1+T$ , thus  $\epsilon_j(T) \leq 2T+1$ , which is at most  $MT^{1/2} \log T$  if we choose  $M \geq (2T+1)T^{-1/2} / \log T$ .

Assume the induction hypothesis for  $t \geq T$ , which means that  $|\epsilon_j(t)| \leq Mt^{1/2} \log t$  for all  $j \leq k$ . We will prove that  $|\epsilon_j(t+1)| \leq M(t+1)^{1/2} \log(t+1)$  for all  $j \leq k$ .

From Eq. (18), we have:

$$\epsilon_j(t+1) \leq \left( 1 - \frac{A_j}{\lambda t} \right) \epsilon_j(t) + \frac{A_{j-1}}{\lambda t} \epsilon_{j-1}(t) + Lt^{-1/2} \log t. \quad (20)$$

If we choose  $T \geq t_1 := \lceil \max_{j:j \leq k} A_j/\lambda \rceil$ , then  $1 - A_j/(\lambda t) \geq 0$  for all  $j \leq k$  and  $t \geq T$ . Thus from the induction hypothesis, Eq. (20) leads to:

$$\begin{aligned} \epsilon_j(t+1) &\leq \left(1 - \frac{A_j}{\lambda t} + \frac{A_{j-1}}{\lambda t}\right) Mt^{1/2} \log t + Lt^{-1/2} \log t. \\ &= Mt^{1/2} \log t + (L - A_j M/\lambda + A_{j-1} M/\lambda) t^{-1/2} \log t. \end{aligned} \quad (21)$$

Notice that, when  $a \leq 1/4$ , the following inequality holds for all  $t \geq 1$ :

$$t^{1/2} \log t + at^{-1/2} \log t \leq (t+1)^{1/2} \log(t+1). \quad (22)$$

Thus, when  $M \geq 4L$ , Eqs. (21) and (22) lead to:

$$\begin{aligned} \epsilon_j(t+1) &\leq Mt^{1/2} \log t + (L - A_j M/\lambda + A_{j-1} M/\lambda) t^{-1/2} \log t \\ &= M \left( t^{1/2} \log t + \left( \frac{L}{M} - A_j/\lambda + A_{j-1}/\lambda \right) t^{-1/2} \log t \right) \\ &\leq M(t+1)^{1/2} \log(t+1), \end{aligned} \quad (23)$$

since  $-A_j/\lambda + A_{j-1}/\lambda \leq 0$ .

By symmetry, when  $M \geq 4L$ , one will also have  $\epsilon_j(t+1) \geq -M(t+1)^{1/2} \log(t+1)$  for all  $j \leq k$  and  $t \geq T$ . So the induction is complete if we choose  $T = \max\{t_0, t_1\}$ , with  $t_1 = \lceil \max_{j:j \leq k} A_j/\lambda \rceil$ , and  $M = \max\{4L, (2T+1)T^{-1/2}/\log T\}$ . This completes the proof of Proposition 1.

## B Additional details on PAFit-oneshot

The unbinned version of PAFit-oneshot can be described as in Fig. 6.

We discuss how to use PAFit-oneshot with binning. Suppose that we have  $J$  bins  $B_1, \dots, B_J$ , each bin is a non-overlapping set of contiguous degrees, i.e.,  $B_g = \{k_g, k_g + 1, \dots, k_g + l_g - 1\}$  with  $l_g$  is the length of the  $g$ -th bin. Binning as a regularization technique works by enforcing the same PA value for all the degree  $k$  in a bin, that is,  $\theta_g = A_k$  for all  $k \in B_g$ . This regularization trades fine details of the PA function for a reduction in the number of parameters needed to be estimated.

For binning, we have the following theorem, whose proof is omitted since it is similar to the proof of Theorem 1:

### Theorem 2

*Assume the same conditions as in Theorem 1. Suppose that  $\theta_g = A_k$  for all  $k \in B_g$ .*

*We have:*

$$\theta_g = \lambda \frac{\mathbb{E} \sum_{k \in B_g} \sum_{j \geq k} n_k(t)}{\sum_{k \in B_g} \mathbb{E} n_k(t)} + o(1). \quad (24)$$

Plugging  $t = T$  into Eq. (24) and correcting for the bias when we observe  $G_T$ , we obtain:

$$\theta_g \approx \frac{\sum_{k \in B_g} \sum_{j \geq k} n_k(T)}{\sum_{k_1 \in B_g: n_{k_1}(T) > 0} n_{k_1}(T) \mathbb{P}(n_{k_1}(T) > 0)}. \quad (25)$$

```

Input:  $G$ ,  $M$ , and  $S$ 
Output:  $\hat{A}_k$  and its standard deviation  $sd(\hat{A}_k)$ 
begin
  Let  $E$ ,  $N$  be the numbers of edges and nodes in  $G$ , respectively
  Let  $T = E + N - 1$  and  $\hat{p} = (N - 2)/(E + N - 2)$ 
  Calculate  $\hat{A}_k^{(0)} = \hat{A}_k^{\text{baseline}}$ , which is given by Eq. (3)
  for  $s = 1, \dots, S$  do
    for  $i = 1, \dots, M$  do
      Simulate a SG model network with  $T$  time-steps,  $p(t) = \hat{p}$ , and  $\hat{A}_k^{(s-1)}$  as the PA function
      Calculate  $p_k^{(s,i)}$  by Eq. (5)
    end
    Calculate  $\hat{p}_k^{(s)}$  by Eq. (6)
    for  $k = 0, \dots, K$  do
      if  $\hat{p}_k^{(s)} > 0$  then
        Calculate  $\hat{A}_k^{(s)}$  by Eq. (7)
      else
         $\hat{A}_k^{(s)} = 0$ 
      end
    end
  end
  Calculate  $\hat{p}_k$  by Eq. (8)
  Repeat the process five times to obtain five values of  $\hat{p}_k$ . Denote their average  $\hat{p}_k^{\text{final}}$ 
  Calculate  $sd(\hat{p}_k^{\text{final}})$ , the standard deviation of  $\hat{p}_k^{\text{final}}$ , from all the samples  $\{p_k^{(s,i)}\}$ 
  for  $k = 0, \dots, K$  do
    if  $\hat{p}_k^{\text{final}} > 0$  then
      Calculate  $\hat{A}_k$  by Eq. (9)
      Calculate  $sd(\hat{A}_k) = sd(\hat{p}_k^{\text{final}}) \sum_{j>k} n_k(T)/n_k(T)/\hat{p}_k^{\text{final}^2}$ 
    else
       $\hat{A}_k = 0$ 
    end
  end
end

```

Figure 6: The workflow of PAFit-oneshot.

At each round  $s$ , the estimate of  $\theta_g$  is:

$$\hat{\theta}_g^{(s)} = \frac{\sum_{k \in B_g} \sum_{j > k} n_k(T)}{\sum_{k_1 \in B_g: n_{k_1}(T) > 0} n_{k_1}(T) \hat{p}_{k_1}^{(s)}}, \quad (26)$$

where  $\hat{p}_k^{(s)}$  is given by Eq. (6). The final estimate of  $\theta_g$  is:

$$\hat{\theta}_g = \frac{\sum_{k \in B_g} \sum_{j > k} n_k(T)}{\sum_{k_1 \in B_g: n_{k_1}(T) > 0} n_{k_1}(T) \hat{p}_{k_1}^{\text{final}}}. \quad (27)$$

## C Maximum Likelihood Estimation when time-resolved data is available

Here we present the MLE in the case when the growth process of the network is completely observed. This MLE serves as a gold standard for evaluating how well various methods perform in networks with time-resolved data.

We assume that we have time-resolved data, which means that we obtain  $G_1, G_2, \dots, G_T$ . The log-likelihood function is:

$$l(\mathbf{A}) = \sum_{t=1}^{T-1} \sum_{k=0}^K m_k(t) \log A_k - \sum_{t=1}^{T-1} m(t) \log \sum_{j=0}^K n_j(t) A_j, \quad (28)$$

with  $\mathbf{A} = [A_0, A_1, \dots, A_K]$  the parameter vector we need to estimate,  $n_k(t)$  the number of nodes with degree  $k$  at the onset of time-step  $t$ , and  $m_k(t)$  the number of new edges connecting to a degree  $k$  node at  $t$ . Here  $K$  is the maximum degree to have appeared in the growth process. We note that  $\mathbf{A}$  is only identifiable up to a multiplicative constant, so in practice one often normalizes  $\mathbf{A}$  so that  $A_1 = 1$ . When the scale of  $\mathbf{A}$  is fixed, the log-likelihood function is known to be concave [28]. Solving the first-order optimality condition for this function leads to the following maximum likelihood equation:

$$A_k = \frac{\sum_{t=1}^{T-1} m_k(t)}{\sum_{t=1}^{T-1} m(t) \frac{n_k(t)}{\sum_j n_j(t) A_j}}. \quad (29)$$

Although a closed-form solution of this equation is unknown, the equation can be used as an update scheme that converges to the maximum likelihood estimator [28].

## D Additional simulation results

Figures 7 and 8 show the result when we use  $A_k = \max(k, 1) / (1 + \beta \log(\max(k, 1)))$  as the true PA function for the case when  $p(t)$  is held fixed and the case when  $p(t)$  is varied based on real-world data. This functional form has been used in modelling

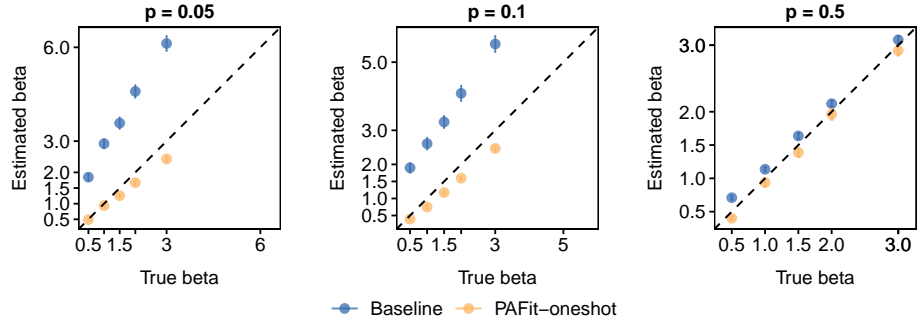


Figure 7: Simulation with  $T = 5 \times 10^5$  and  $A_k = \max(k, 1) / (1 + \beta \log(\max(k, 1)))$ . For each case,  $p(t) = p$ , i.e., a constant. In each setting, the number of simulations is 50.

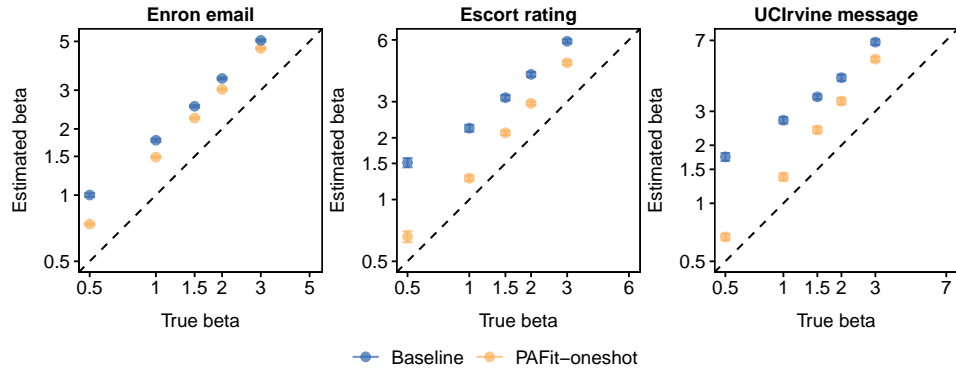


Figure 8: Simulation with real-world node-edge sequences obtained from three real-world networks and  $A_k = \max(k, 1) / (1 + \beta \log(\max(k, 1)))$ . This PA form has been used in modelling citations in physics [33]. In each setting, the number of simulations is 50.

citations in physics [33]. The results show that the proposed method outperformed the baseline with this PA function too.

For the results in Fig. 3, Figure 9 shows two runs that are typical for the situations when  $\alpha$  is small and when  $\alpha$  is large, respectively.

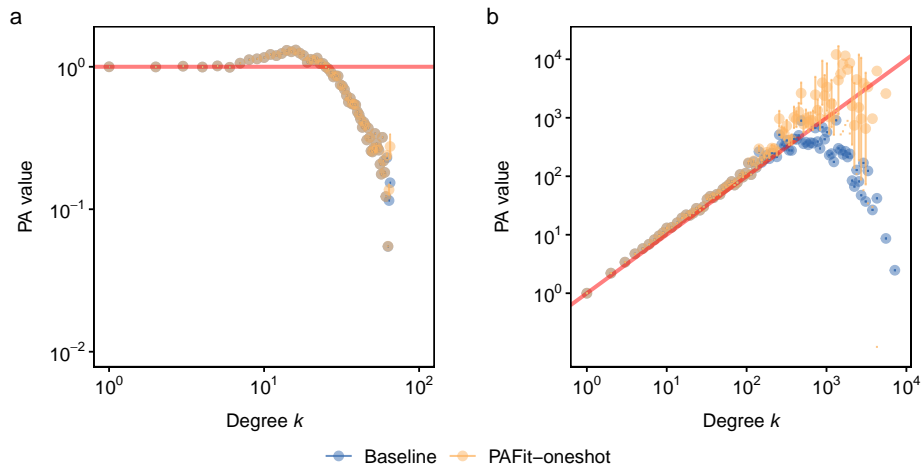


Figure 9: Two typical runs in simulations with Enron email network when we use  $A_k = \max(k, 1)^\alpha$ . **Panel a:**  $A_k = 1$  ( $\alpha = 0$ ). PAFit-oneshot failed to remove the waterfall artefact. **Panel b:**  $A_k = k$  ( $\alpha = 1$ ). PAFit-oneshot corrected the waterfall artefact and gave good estimation values.

## E Additional information for real-world networks with time-resolved data

Table 2 shows several statistics for the networks in Fig. 4.

Table 2: Summary statistics of networks with time-resolved data.  $N$  and  $E$  is the number of nodes and edges, respectively.  $T$  is the number of time-steps.  $\bar{p}$  is the average ratio of nodes.  $d_{max}$  is the maximum degree in the network.

Network	$N$	$E$	$T = N + E - 1$	$\bar{p} = N/T$	$d_{max}$
Enron email	87272	1148072	1235343	0.07	5419
Sexual escort rating	6624	50632	57255	0.12	615
UCIrvine forum message	1899	59835	61733	0.03	1546

Figure 10 show the estimated  $p(t)$  in the three real-world networks.

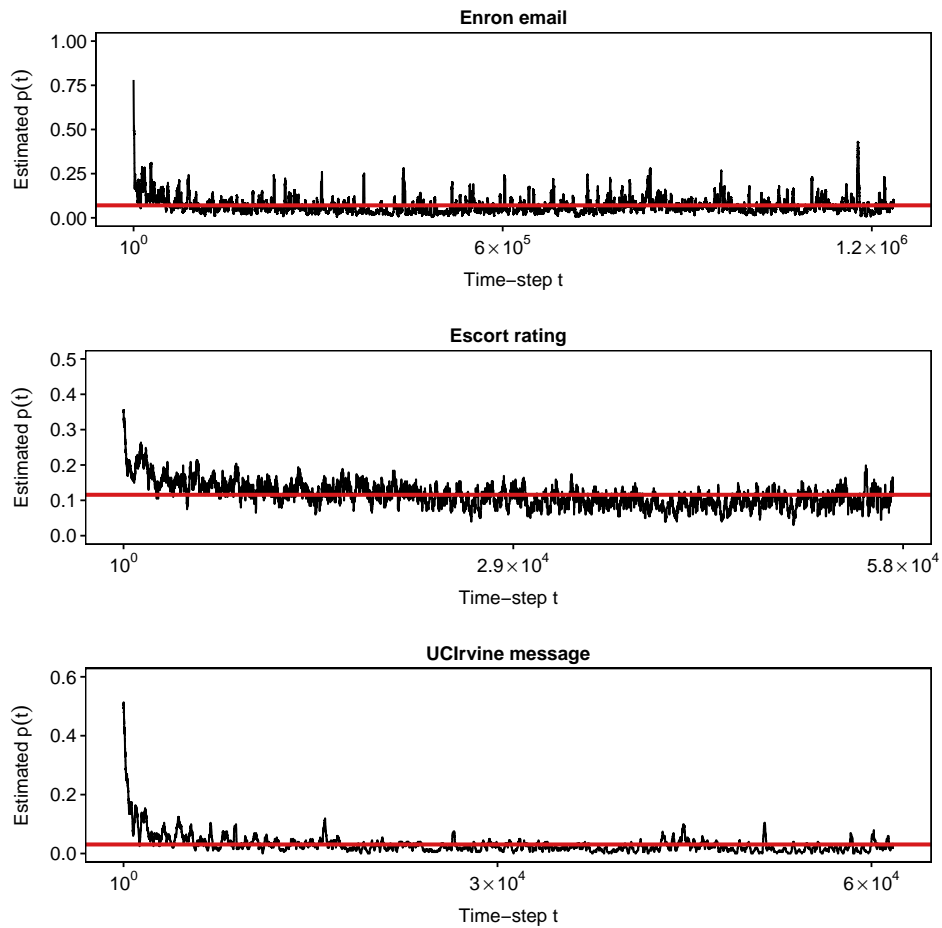


Figure 10: Estimated  $p(t)$  in three real-world networks with time-resolved data: Enron email, the Escort rating, and the UC Irvine forum message networks. At each time-step  $t$ , we estimate  $p(t)$  by the average of the number of time-steps that contains a new node in the range  $t \pm 500$  in the Enron email network and  $t \pm 50$  in the Sexual escort rating and the UC Irvine forum message networks. The horizontal red lines indicate the average  $\bar{p}$  in the networks, whose values can be found in Table 2.

## F Additional information for real-world networks without time-resolved data

Table 3 shows several statistics for the networks in Fig. 5. The degree distributions are given in Fig. 11. The scale-free form is fitted to the empirical degree distribution by method of Clauset [9].

Table 3: Several statistics for the real-world networks with no time-step information.  $N$  and  $E$  is the number of nodes and edges, respectively.  $\bar{p}$  is the average ratio of nodes.  $d_{max}$  is the maximum degree in the network.

Network	$N$	$E$	$\bar{p} = N/(N + E)$	$d_{max}$
US Airports	6624	50632	0.12	615
Google+	23628	39242	0.38	26
2004 US Election blogs	1224	19025	0.06	467

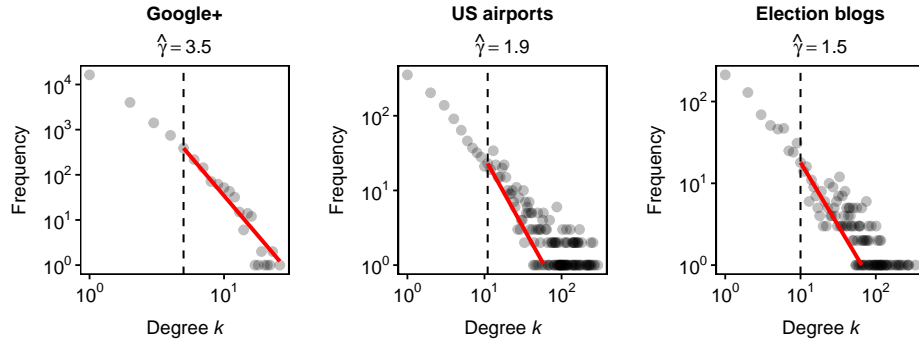


Figure 11: Degree distributions of real-world networks with no time-step information. The power-law exponent  $\gamma$  is estimated by maximum likelihood estimation. The degree threshold  $k_{min}$  from which the power-law property holds is estimated by Clauset method in the Google+ and US airport networks. They are  $k_{min} = 11$  and  $k_{min} = 5$ , respectively. In the Election blog network,  $k_{min} = 10$  is chosen by visual inspection.

## References

- [1] Adamic, L. A. & Glance, N. (2005) The Political Blogosphere and the 2004 U.S. Election: Divided They Blog. In *Proceedings of the 3rd International Workshop on Link Discovery*, LinkKDD '05, page 36–43, New York, NY, USA. Association for Computing Machinery.
- [2] Albert, R. & Barabási, A. (1999) Emergence of Scaling in Random Networks. *Science*, **286**, 509–512.

- [3] Alves, C., Ribeiro, R. & Sanchis, R. (2021) Preferential Attachment Random Graphs with Edge-Step Functions. *Journal of Theoretical Probability*, **34**(1), 438–476.
- [4] Bezáková, I., Kalai, A. & Santhanam, R. (2006) Graph Model Selection Using Maximum Likelihood. In *Proceedings of the 23rd International Conference on Machine Learning, ICML '06*, pages 105–112, New York, NY, USA. ACM.
- [5] Bhamidi, S. (2007) Universal techniques to analyze preferential attachment trees: Global and Local analysis. .
- [6] Bradford, S. C. (1985) Sources of Information on Specific Subjects. *J. Inf. Sci.*, **10**(4), 173–180.
- [7] Cantwell, G. T., St-Onge, G. & Young, J.-G. (2021) Inference, Model Selection, and the Combinatorics of Growing Trees. *Phys. Rev. Lett.*, **126**, 038301.
- [8] Clauset, A., Shalizi, C. & Newman, M. (2009a) Power-Law Distributions in Empirical Data. *SIAM Review*, **51**(4), 661–703.
- [9] Clauset, A., Shalizi, C. R. & Newman, M. E. J. (2009b) Power-Law Distributions in Empirical Data. *SIAM Review*, **51**(4), 661–703.
- [10] Dereich, S. & Mörters, P. (2009) Random networks with sublinear preferential attachment: Degree evolutions. *Electron. J. Probab.*, **14**, 1222–1267.
- [11] Gao, F., van der Vaart, A., Castro, R. & van der Hofstad, R. (2017) Consistent estimation in general sublinear preferential attachment trees. *Electron. J. Statist.*, **11**(2), 3979–3999.
- [12] Gillespie, C. (2015) Fitting Heavy Tailed Distributions: The poweRlaw Package. *Journal of Statistical Software, Articles*, **64**(2), 1–16.
- [13] Guetz, A. N. & Holmes, S. P. (2011) Adaptive importance sampling for network growth models. *Annals of Operations Research*, **189**(1), 187–203.
- [14] Hagberg, O. & Wiuf, C. (2006) Convergence properties of the degree distribution of some growing network models. *Bulletin of Mathematical Biology*, **68**(6), 1275.
- [15] Jeong, H., Néda, Z. & Barabási, A. (2003) Measuring preferential attachment in evolving networks. *Europhysics Letters*, **61**(61), 567–572.
- [16] Klimt, B. & Yang, Y. (2004) The Enron corpus: A new dataset for email classification research. In *In Proc. European Conf. on Machine Learning*, pages 217–226.
- [17] Krapivsky, P., Rodgers, G. & Redner, S. (2001a) Degree Distributions of Growing Networks. *Physical Review Letters*, **86**(23), 5401–5404.
- [18] Krapivsky, P., Rodgers, G. & Redner, S. (2001b) Organization of growing networks. *Physical Review E*, page 066123.

- [19] Leskovec, J. & McAuley, J. (2012) Learning to Discover Social Circles in Ego Networks. In Pereira, F., Burges, C. J. C., Bottou, L. & Weinberger, K. Q., editors, *Advances in Neural Information Processing Systems*, volume 25, pages 539–547. Curran Associates, Inc.
- [20] Lima-Mendez, G. & van Helden, J. (2009) The powerful law of the power law and other myths in network biology. *Mol. BioSyst.*, **5**, 1482–1493.
- [21] Lotka, A. J. (1926) The frequency distribution of scientific productivity. *Journal of the Washington Academy of Sciences*, **16**(12), 317–323.
- [22] Lü, L. & Zhou, T. (2011) Link prediction in complex networks: A survey. *Physica A: Statistical Mechanics and its Applications*, **390**(6), 1150–1170.
- [23] Merton, R. K. (1968) The Matthew Effect in Science. *Science*, **159**(3810), 56–63.
- [24] Newman, M. (2001) Clustering and preferential attachment in growing networks. *Physical Review E*, **64**(2), 025102.
- [25] Opsahl, T. (2011) Why Anchorage is not (that) important: Binary ties and Sample selection. <https://toreopsahl.com/2011/08/12/why-anchorage-is-not-that-important-binary-ties-and-sample-selection/>.
- [26] Opsahl, T. & Panzarasa, P. (2009) Clustering in Weighted Networks. *Social Networks*, **31**, 155–163.
- [27] Perc, M. (2014) The Matthew Effect in Empirical Data. *Journal of The Royal Society Interface*, **11**(98).
- [28] Pham, T., Sheridan, P. & Shimodaira, H. (2015) PAFit: a Statistical Method for Measuring Preferential Attachment in Temporal Complex Networks. *PLOS ONE*, **10**(9), e0137796.
- [29] Pham, T., Sheridan, P. & Shimodaira, H. (2016) Joint Estimation of Preferential Attachment and Node Fitness in Growing Complex Networks. *Scientific Reports*, **6**.
- [30] Pham, T., Sheridan, P. & Shimodaira, H. (2020) PAFit: An R Package for the Non-Parametric Estimation of Preferential Attachment and Node Fitness in Temporal Complex Networks. *Journal of Statistical Software, Articles*, **92**(3), 1–30.
- [31] Price, D. d. S. (1965) Networks of Scientific Papers. *Science*, **149**(3683), 510–515.
- [32] Price, D. d. S. (1976) A general theory of bibliometric and other cumulative advantage processes. *Journal of the American Society for Information Science*, **27**, 292–306.
- [33] Redner, S. (2005) Citation statistics from 110 years of physical review. *Physics Today*, **58** (6), 49–54.

- [34] Rocha, L. E. C., Liljeros, F. & Holme, P. (2010) Information dynamics shape the sexual networks of Internet-mediated prostitution. *Proceedings of the National Academy of Sciences*, **107**(13), 5706–5711.
- [35] Rodgers, G. & Zheng, D. (2002) A herding model with preferential attachment and fragmentation. *Physica A: Statistical Mechanics and its Applications*, **308**(1), 375–380.
- [36] Rudas, A., Tóth, B. & Valkó, B. (2007) Random trees and general branching processes. *Random Structures & Algorithms*, **31**(2), 186–202.
- [37] Serafino, M., Cimini, G., Maritan, A., Rinaldo, A., Suweis, S., Banavar, J. R. & Caldarelli, G. (2021) True scale-free networks hidden by finite size effects. *Proceedings of the National Academy of Sciences*, **118**(2).
- [38] Sheridan, P., Yagahara, Y. & Shimodaira, H. (2012) Measuring preferential attachment in growing networks with missing-timelines using Markov chain Monte Carlo. *Physica A Statistical Mechanics and its Applications*, **391**, 5031–5040.
- [39] Simon, H. A. (1955) On a Class of Skew Distribution Functions. *Biometrika*, **42**(3-4), 425–440.
- [40] Taylor, J. & Tibshirani, R. J. (2015) Statistical learning and selective inference. *Proceedings of the National Academy of Sciences*, **112**(25), 7629–7634.
- [41] Tibshirani, R. J., Taylor, J., Lockhart, R. & Tibshirani, R. (2016) Exact Post-Selection Inference for Sequential Regression Procedures. *Journal of the American Statistical Association*, **111**(514), 600–620.
- [42] Virkar, Y. & Clauset, A. (2014) POWER-LAW DISTRIBUTIONS IN BINNED EMPIRICAL DATA. *The Annals of Applied Statistics*, **8**(1), 89–119.
- [43] Wan, P., Wang, T., Davis, R. A. & Resnick, S. I. (2017) Fitting the linear preferential attachment model. *Electron. J. Statist.*, **11**(2), 3738–3780.
- [44] Wan, P., Wang, T., Davis, R. A. & Resnick, S. I. (2019) Are extreme value estimation methods useful for network data?. *Extremes*.
- [45] Wang, T. & Resnick, S. I. (2019) Consistency of Hill estimators in a linear preferential attachment model. *Extremes*, **22**(1), 1–28.
- [46] Yule, G. U. (1925) A Mathematical Theory of Evolution, Based on the Conclusions of Dr. J.C. Willis, F.R.S.. *Philosophical Transactions of the Royal Society of London B: Biological Sciences*, **213**(402-410), 21–87.